PAPER

Polyglycerol resin towards sustainable 3D-printing†

Katherine George,‡[a] Eduards Krumins,‡[a] Eileen Tan,[b] Yinfeng He, [ID] [ac] Ricky Wildman,[a] Robert Owen, [ID] [b] Joel Segal,*[d] Valentina Cuzzucoli Crucitti*[e] and Vincenzo Taresco [ID] *[f]

Additive manufacturing (AM) techniques, also named three-dimensional (3D)-printing, have been widely recognised as promising technologies for rapid production of novel, personalised drug-delivery systems and scaffolds for biofabrication, and in food applications and many more fields. Although there has been promising progress in identifying new materials for 3D-printing, the range of resins/polymers available is still limited, with big reliance on petroleum-derived materials and the advancement is not up to date with the fast-developing hardware. Therefore, new building blocks that are renewably sourced and biodegradable are desirable for expanding applicability and recyclability. Specifically, glycerol, a readily available waste product from biodiesel processing, is highly functionalisable since it bears three hydroxyl groups. We previously reported that an acrylated glycerol-based oligomer, polyglycerol-6-acrylate, fulfils all the necessary criteria for volumetric printing (transparency, photo-reactivity and viscosity) and was successfully used to print a variety of models with intricate geometries and good resolution. In the present work, we want to expand the use of (meth)acrylated-polyglycerols (4 and 6 units of glycerol) to stereolithography (SLA), as this technique presents numerous advantages, being also more commercially available. Printability parameters, different geometries, and biocompatibility are explored to confirm the amenability of SLA to these "greener" resins. In addition, as initial proof of concept, the replacement of (meth)acrylate moieties is explored by ring opening of

[a]Centre for Additive Manufacturing, Department of Chemical and Environmental Engineering, Faculty of Engineering, University of Nottingham, Nottingham, NG7 2RD, UK

[b]School of Pharmacy, Biodiscovery Institute, University of Nottingham, Nottingham, NG7 2RD, UK

[c]Nottingham Ningbo China Beacons of Excellence Research and Innovation Institute, University of Nottingham Ningbo China, Ningbo 315100, China

[d]Advanced Manufacturing Technology Research Group, Faculty of Engineering, University of Nottingham, University Park, Nottingham NG7 2RD, UK. E-mail: joel.segal@nottingham.ac.uk

[e]Department of Chemical and Environmental Engineering, Faculty of Engineering, University of Nottingham, University Park, Nottingham NG7 2RD, UK. E-mail: valentina.cuzzucolicrucitti1@nottingham.ac.uk

[f]School of Chemistry, University of Nottingham, Nottingham, NG7 2RD, UK. E-mail: vincenzo.taresco@nottingham.ac.uk

† Electronic supplementary information (ESI) available. See DOI: https://doi.org/10.1039/d5fd00043b

‡ Authors contributed equally.

maleic and norbornene anhydrides in order to achieve acrylic-free resins and preliminary curability tests on these bioderived resins were performed. By developing and testing these new acrylic/acrylic-free resins based on glycerol, we aim to accelerate the adoption of greener alternatives in AM, contributing to a more sustainable future in the 3D-printing world.

Introduction

The concept of the additive manufacturing (AM) technique was developed in 1986 by Charles Hull, who invented and later commercialised and patented the first 3D printer, based on a technique known as stereolithography (SLA).[1] As shown in Fig. 1, the SLA system normally includes an XY scanning mirror, a resin tank, a construction platform, and an ultraviolet (UV) laser source.[1,2] SLA has the capability to generate thin features ($\simeq 10$ μm) and can reach intricate geometries, with high reliability[1,3,4] and reduced waste production. However, SLA printing has some limitations, such as expensive and limited types of photocurable resins.[5,6]

A specific concern relates to the limited availability of sustainable resins that have the required photoreactive chemistry for printing.[8] Current research has shown the future direction in sustainability with the use of both renewable feedstocks and waste feedstocks for SLA materials by eliminating the reliance on petroleum-based materials.[8–11] Numerous alternatives derived from cellulose, terpenes, lignin and other sources have been explored;[12–14] nevertheless, the predominant share of commercial materials continues to rely on petrochemicals.

Glycerol, a by-product of the biodiesel and soap industries, is obtained on a large scale, with production anticipated to exceed 4 billion litres in 2026.[15] By 2030, crude glycerol output is projected to exceed four billion gallons annually, equivalent to 49 882 million litres, as reported by the Organisation for Economic Co-operation and Development (OECD).[16] Additionally, glycerol
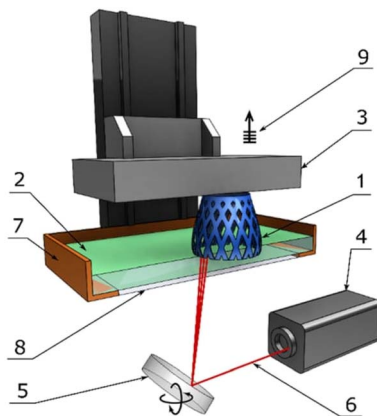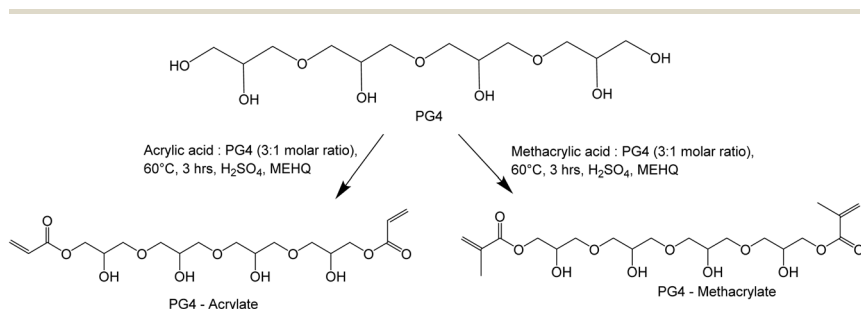

Fig. 1 Components of a typical SLA machine: 1—printed part, 2—liquid resin, 3—building platform, 4—UV laser source, 5—XY scanning mirror, 6—laser beam, 7—resin tank, 8—window, and 9—layer-by-layer elevation.[7]

constitutes approximately 10% of the overall conversion output of biodiesel production.[17,18] The polymerisation of glycerol to create oligomeric poly-glycerols (PGs) is one way to valorise it. The end product is a hydrophilic, viscous, transparent polyol that is verified to be easily biodegradable.[19,20] Oligomeric PGs have been used as humectants in personal care products, medicinal additives, and more.[21]

Previously, we published the development of a sustainable photocurable resin based on polyglycerols (PGs) for volumetric additive manufacturing (VAM).[22] The current work expands on this by demonstrating the use of stereolithography (SLA) printing as a proof-of-concept to establish PG-based materials as a sustainable platform for a variety of vat photopolymerization techniques, including both SLA and VAM. Notably, SLA is a well-established and widely adopted printing technology, already present in many households and used daily by non-specialist users, highlighting its potential for scalable deployment of sustainable resins. Given that VAM is a relatively recent innovation, introduced in 2017, using SLA as a complementary technique serves to strengthen the accessibility and versatility of PG-based materials.[23] Furthermore, PG—being a by-product of biodiesel production—represents a prime example of how low-value waste streams can be upcycled into high-value, next-generation resin systems for additive manufacturing.

In the present study, we report the synthesis of a series of curable acrylated and methacrylated resins derived from PG, formed by an average of 4 and 6 glycerol units (Scheme 1). We demonstrate for the first time the successful fabrication of complex structures across all resin types using commercial SLA printers, underscoring both the robustness of the PG-based resins and the flexibility of SLA hardware to accommodate different resin viscosities and chemistries. We also demonstrate the biocompatibility of the printed polymers when suitably post-processed. This highlights the practical potential of PG-derived materials for broad, real-world use. In support of sustainable additive manufacturing goals, we also explored alternatives to conventional (meth)acrylate modifications by introducing maleic and norbornene moieties into PG side chains. These alternative chemistries could open doors for applications in tissue engineering and regenerative medicine as biodegradable and biocompatible alternatives to established materials like gelatin methacrylate. Preliminary screenings indicate the curability of these novel PG modifications, furthering the promise of a waste-to-resource model for resin innovation.

Scheme 1 Synthesis of PG4–acrylate (PG4–A) and PG4–methacrylate (PG4–MA).

Results and discussion

Resin synthesis optimisations and resin characterisation

A direct Fischer esterification method using acrylic acid and catalytic sulfuric acid (Scheme 1) was employed to functionalise polyglycerol with acrylate groups, making the material photocurable.[24]

The molar ratios between PG and the curable functionalities were screened to find the optimal conditions for balancing reactivity and curability, while minimising the use of (meth)acrylate molecules. It was found that using an acrylic acid : PG4 molar ratio of 2 : 1 resulted in a conversion rate of approximately 30%, indicating less than one acrylate per chain. During UV-curing screening, no insoluble solid scaffold was formed, likely due to the formation of a linear polymer rather than a crosslinked network. This formation is attributed to the low ratio and conversion, showing PG4 rather as a mono-acrylate oligomer.

The significance of this was evident when printed scaffolds were placed in 1 M NaOH, leading to their breakdown within 5 minutes. This indicated the formation of acrylic sodium salt with NaOH, which reduced hydrogen bonds (between PG and polyacrylic acid), increasing the solubility of the entire system due to the presence of a linear polymer. In fact, linear polymer chains can exhibit physical crosslinking, including non-covalent bonds such as hydrogen bonding. Due to limited chemical crosslinking, the printed scaffolds are weak and undergo hydrolysis/solubilisation quickly.

The use of acrylic acid : PG4 with a 3 : 1 molar ratio was used to overcome this issue and improve conversion results and chemical crosslinking within the structure. The calculated conversion using ^{1}H-NMR was approximately 62%, indicating over one acrylate per chain (^{1}H-NMR analysis section in the ESI†). Therefore, a greater number of acrylates with reactive double bonds are available for chemical crosslinking, when exposed to the UV light during printing. As the crosslinking increases, a more extensive 3D network is formed after curing, which leads to a rigid sample. In comparison to the 2 : 1 molar ratio, the printed scaffold began to break down after approximately 25 minutes in 1 M NaOH, indicating an increased stability due to a more extended chemical crosslinking network within the scaffold and a reduced amount of free polyacrylic acid. On the other hand, the conversion of methacrylic acid in PG4–MA (1 : 3 ratio) was estimated to be around 30% (*ca.* one double bond per chain); however, due to the different chemical nature of the methacrylate moieties, solid structures could be produced after UV-curing. Both the virgin and the meth(acrylated) PG4/PG6 macromolecules are amorphous and viscous liquids. Dynamic mechanical analysis (DMA) of all the printed scaffolds, from any of the resins, showed low values of T_g ranging from −6 to 6 °C (Table 1), indicating that the printed samples are highly crosslinked structures. The T_g value for PG4–A was slighter higher than that of PG6–MA due to the higher crosslinking density as there is a greater number of acrylates per chain in comparison to MA samples.[25] The virgin PG4 was shown to be thermally stable with a single weight loss step centred at around 370 °C, while PG4 acrylate showed three additional weight loss transitions at around 150–200 °C, 230–260 °C and around 400–425 °C (TGA analysis in the ESI†). These steps may be due to the presence of free and bound acrylic acid plus some residual water (from the catalyst and humidity) and additional reagents and catalyst degradation. PG6 was

Table 1 Properties of PG–(meth)acrylate samples, NA = not applicable, ND = not determined. See ESI for TGA traces

Sample	Conversion[a]	Viscosity [b] at 25 °C (Pa s)	T_g^c (°C)
PG4–A (1 : 3)	65 ± 5%	20	−2
PG4–MA (1 : 3)	30 ± 5%	2	−13
PG6–A (1 : 3)	65 ± 5%	28	6
PG6–MA (1 : 3)	30 ± 5%	4	−6

[a] Average over two batches. [b] Calculated as the average from 1–1000 s^{-1}. [c] From tan delta peak at 1 Hz.

shown to be thermally stable with a single weight loss step centred at around 350 °C, while PG6 acrylate and methacrylate showed three weight loss transitions at around 175–190 °C, around 250 °C and the last one around 400–425 °C. Again, these two steps may be due to the presence of free and bound acrylic acid plus some residual water (from the catalyst and humidity) and additional reagents and catalyst degradation.

Although viscosity values suitable for SLA resins should remain below 5 Pa s,[26,27] there are commercially available resins for SLA with viscosities up to 10 Pa s, which offer improved mechanical properties.[28,29] In our case, the viscosity of PG4-A/MA and PG6-A/MA ranged from 2 to 28 Pa s when measured at an average temperature of 25 °C (Table 1). Considering that the initial viscosities of the unfunctionalised PG4 and PG6 are 64 and 120 Pa s, respectively, the (meth)acrylation process clearly reduced the hydrogen bonding between the hydroxyl groups of the PG chains, indicating an ability to alter the final viscosity. In the literature, such high-viscosity resins are typically printed by adding a viscosity modifier or by modifying the printer hardware.[30–32] Positively, in our case, the unreacted (meth)acrylate functionalities acted as viscosity modifiers, reducing the overall viscosity of the PG resin formulations and enhancing printability in the vat of the SLA printer. In particular, methacrylic samples showed lower viscosity as a higher amount of free methacrylic acid remained free, favouring the overall flowability of the resin under shear. However, other variables may have synergistically affected the printability of our resins in an unaltered SLA printer despite their high viscosity. It can be speculated that, in addition to the aforementioned effects, the low glass transition temperatures (T_gs) of the polyglycerol-based materials and a prompt temperature increase (recorded in our SLA system up to 55 °C) positively influenced the fluidity of the resin, resulting in a high printability response.

Curability and printability tests

Once the homogeneous resin was produced (PG-functionalised polymer and photoinitiator), a drop was placed onto a microscope slide and cured under UV light (wavelengths 365 and 405 nm) in 10-second increments to determine the estimated cure-time per layer. Once the estimated cure-time was determined, a printability test using the SLA printer was conducted.

The printability test was performed by printing a rectangular scaffold with a circular extrusion in the top right corner of each square (Fig. 2). Each layer was
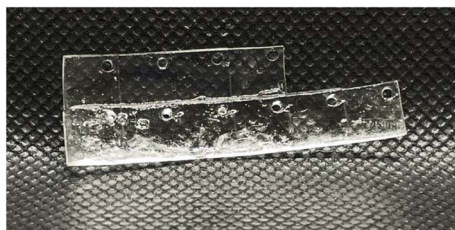
Fig. 2 Initial exposure scaffold to determine normal layer exposure for PG4–A.

Table 2 Simple and complex SLA-printed geometries

Simple structures	Complex structures
Wide cylinders with a diameter of 10 mm and a height of 3 mm	Rook (Fig. 4)
Narrow cylinders with a diameter of 3 mm and a height of 10 mm	Validation matrix (Fig. 5)
Cube (3 mm and 5 mm)	Boat (Fig. 4)

exposed for 2 seconds, with exposure times ranging from 2 to 40 seconds (corresponding to 1 to 20 layers). After printing, the lowest exposure time at which the extruded circle remained visible was selected as the optimal normal layer exposure time and exhibited high fidelity. A longer exposure time was selected for the base layer to ensure the scaffold adhered to the build plate. For the material PG4–A, the optimal exposure time was identified as 8 seconds per layer. This value changed according to the nature of the resin, as reported in the Methods section of the ESI.†

Once the lowest exposure time was determined, various simple and complex scaffolds, summarised in Table 2 and Fig. 3, were printed.

These structures were chosen because of the presence of basic shapes (cylinders, cubes and pill-like geometry) and more intricate features where higher resolution and resin properties can be probed (like for the rook and the boat).
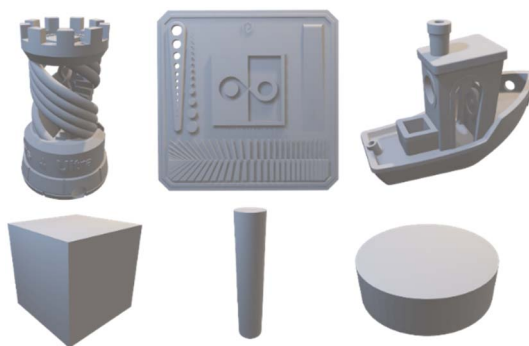

Fig. 3 STL image file of SLA-printed geometries.

Following this determination, both simple and complex geometries were printed using these optimised settings. All of the resins were printed into the broad cylinders and narrow cylinders, as well as the rooks and the boats with good
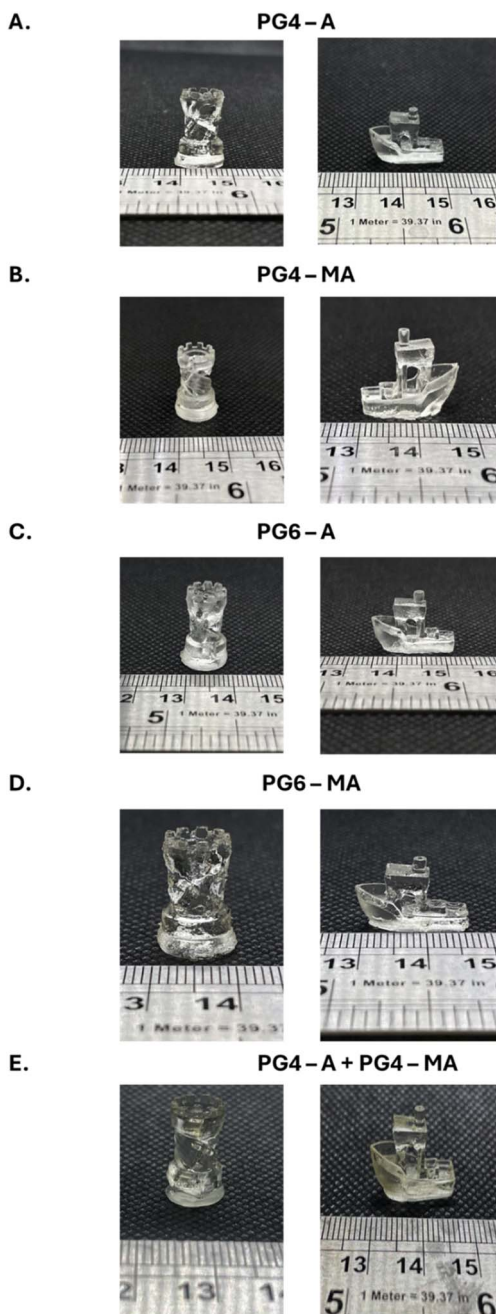

Fig. 4 SLA printing results of (A) PG4−A, (B) PG4−MA, (C) PG6−A, (D) PG6−MA and (E) PG4−A + PG4−MA, representing printed scaffolds, rook and boat, from each resin to test printability.

fidelity compared to the CAD file and good resolution, and forming a self-standing solid system (Fig. 4 and ESI Fig. 6†). Overall, PG4 and PG6 (meth)acrylate resins can be printed using SLA, showing promising visual results in the production of simple and more complex structures.

Finally, a validation matrix with a series of differently spaced and sized features, as well as elaborate patterns and complex orientations, was printed to validate the resins in the system. The validation matrix was used to observe in a more quantitative way the fidelity and any variations of the printed quality from the CAD file, thanks to the measurable features described above and visible in Fig. 5 and ESI Fig. 7.†

Resolution limitations were then examined using the validation matrix structures, which have a variety of geometric characteristics as well as varying sizes of positive and negative features. The infinity symbol's ends should meet precisely, avoiding both overlap (overexposure) and gaps (underexposure). Similarly, the bars should fit snugly into voids without excessive friction, which suggests overexposure, or excessive space, which indicates underexposure. Additionally, the number of pins and holes should be nearly equal, with a slight
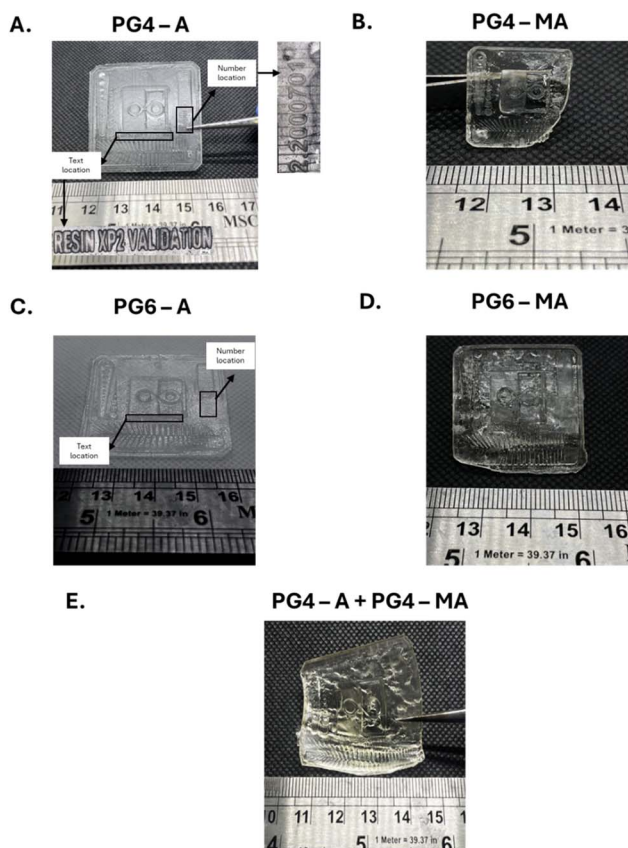

Fig. 5   SLA printing results of validation matrix for (A) PG4−A, (B) PG4−MA, (C) PG6−A, (D) PG6−MA and (E) PG4−A + PG4−MA.

excess of pins signalling overexposure and a slight excess of holes indicating underexposure. The validation matrix, with features ranging from 0.8 mm to 40 mm, allows for assessing and comparing the printability of various resins (Fig. 5). These characteristics include basic forms such as cylinders and rectangles, as well as text and a sequence of numbers.

The PG4–MA samples showed substantially stronger adherence to the base layer, making removal from the build plate difficult. Due to this, the scale of the validation matrix was changed when methacrylates were printed, and supports were necessary to prevent printing directly on the build plate. It was speculated that to tune the printing qualities and minimise the strength of the base adhesion to the build plate, a combination of PG4–A and PG4–MA (50 wt%) could be printed. Despite the fact that the validation matrix was printed on supports, the print scaffold remains warped with subsequent degradation of the quality of the print. This could be likely due to the differences in reactivity and properties of acrylate and methacrylate.

Biocompatibility assessment

With printing parameters established for each resin, test coupons were fabricated from each material for extract biocompatibility testing, with comparison to BioMed Amber (Formlabs), a known biocompatible resin, and 8K Standard Space Grey (ELEGOO), a typical hobbyist 3D printing resin, as material controls. These were post-processed, comparing the effects of an alkali wash to neutralise acidic residues, before performing extract biocompatibility testing (Fig. 6).

Without alkali washing, all PG-based samples demonstrated extract cytotoxicity due to release of acidic residues, as indicated by a cell-culture-medium pH change, an observation in agreement with previous VAM prints.[22] BioMed Amber samples were biocompatible, as expected, whilst Space Grey samples were cytotoxic without any observed acidity. With a 1 M sodium bicarbonate neutralisation prior to extract generation, no visual pH change was observed in the extracted culture media, and all PG-based samples were deemed biocompatible except PG4–MA for being within 30% of the live control. Interestingly, the alkali wash made no significant difference to the biocompatibility of Space Grey. As no pH change was observed, this indicates the release of some other, non-acidic compound from the resin during extract testing, likely the proprietary photoinitiator and/or photoabsorber. It should be noted that alkali treatment did accelerate degradation of the printed samples due to the basic conditions. Methacrylate-based PG resins were observed to better withstand this, best resembling the pre-washed printed part, although acrylate-based PG resins achieved a number of live cells closest to the live control. Overall, if using these 3D-printed PG-based materials for applications where biological interaction is required, the duration of alkali washing to neutralise them requires careful balancing of duration and degradation to ensure biocompatibility and preservation of print fidelity.

Maleic and norbornene anhydride PG modifications

Maleic anhydride (Mal) and norbornene dicarboxylic anhydride (Norb) have been selected as greener curable functionalities to minimise the use of oil and toxic-chemical-based (meth)acrylate functionalities.[33]
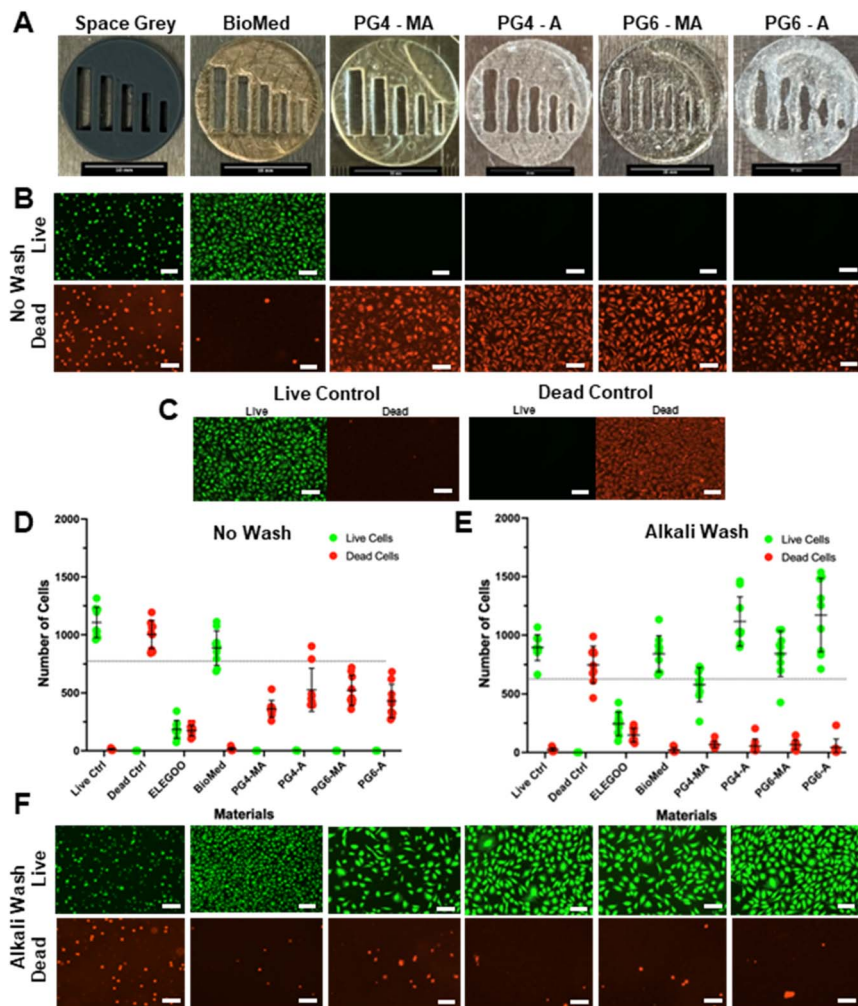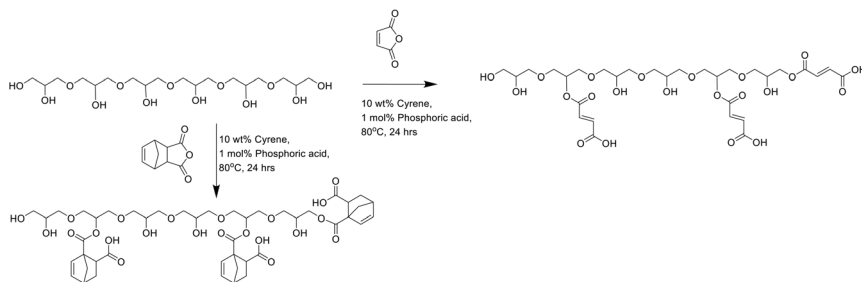
Fig. 6 Extract biocompatibility results. Representative images of (A) test coupons made from each material, (B) live/dead images of cells from non-alkali-washed test-coupon extracts, (C) live/dead images of live and dead control wells, and (D) quantified live/dead staining for non-alkali-washed samples and (E) alkali-washed samples ($N = 3$, $n = 3$). (F) Representative live/dead images of cells from alkali-washed test-coupon extracts. All scale bars: 200 μm.

Mal can be obtained *via* selective transformation of biomass-derived levulinic acid, through a previously reported oxidative scission pathway.[34] Mal could be also sourced from other green platform chemicals such as furfural and 1-butanol.[35,36] At the same time, Norb synthesis from cyclopentadiene and Mal *via* the Diels–Alder reaction is a classical cycloaddition reaction.[37] Mal and Norb are versatile substrates widely used as comonomers (as Mal cannot homopolymerise) and curing agents, and used in the synthesis of monomers for cross-linked polymer networks based on thiol–ene linkages for biomedical applications and coatings.[38–43] Considering the properties of Mal and Norb and their previous

Scheme 2 Reaction strategies to produce PG4-Mal and PG4-Norb, using 10 wt% cyrene to improve reagent solubility and reduce reaction-mixture viscosity.

applications in 3D printing, we utilised these reagents to decorate PG4 and PG6, aiming to produce an ideally "fully sustainable" polymeric resin (Scheme 2) for additive manufacturing.

PG4 and PG6 were functionalised with both reagents, maintaining a Norb/Mal : PG4/6 molar ratio of 3 : 1 (Scheme 2), as deemed the best ratio from the previous set of experiments. Given that both anhydride reagents are solid, a quantity of the bio-based solvent cyrene was added to enhance the solubility of all components and reduce the viscosity of the final reaction mixture, maintaining the concept of green chemistry.[44] Unlike the (meth)acrylation process, the ring opening of the two anhydrides resulted in high conversions, as analysed by ^{1}H-NMR, in the PG hydroxyl group modification, ranging from 86–98% (ESI Fig. 8–11†).[45,46] These high conversions were achieved by using a catalytic amount of phosphoric acid, which enabled up to a 10% increase in conversion compared to the synthesis without free catalyst. Consequently, the functionalised polymers should exhibit a substantial number of free carboxyl groups, providing a significant opportunity to form strong hydrogen bond networks. Cyrene, being a dipolar aprotic solvent with a high boiling point, was further utilised to improve processability by disrupting some of the hydrogen bonding present in the polymer samples. Indeed, the final decorated polymers were highly viscous-to-solid materials, which would have been difficult to remove from the reaction vessels without the presence of cyrene.

The curability of the PG Norb/Mal materials was assessed *via* screening. To achieve curing, a thiol crosslinking agent (trimethylolpropane tris(3-mercaptopropionate)) was added to the PG Norb/Mal materials in varying molar ratios (1 : 1, 2 : 1, and 3 : 1, with respect to the amount of double-bond-containing groups in the PG materials). This strategy is often utilised with maleate- and norbornene-containing macromonomers.[47,48] The screening revealed three materials that cured in a time window suitable for SLA printing (~5 min) (ESI Table 2†). The curable materials were: PG4–Norb (1 : 1), PG6–Mal (1 : 1), and PG6–Norb (1 : 1). Larger monoliths of these materials were then produced *via* photo-polymerization, showcasing that larger structures can be constructed from these materials, indicating their potential for SLA printing (Fig. 7).

Future studies on the processability and printability of these materials could identify the conditions necessary for SLA printing of PG Norb/Mal materials. However, further optimisations are required. Given the high conversion in the

Fig. 7 PG4–Norb (1 : 1) in a larger scaffold produced *via* photo-polymerization.

ring-opening synthesis, a strong physical crosslinking network is anticipated between hydroxyl and carboxyl groups, which reduces solubility, flowability, and the availability and reactivity of double bonds. Additionally, various thiol cross-linkers and vat temperatures, shorter PG chains, and different initiators should be evaluated to determine the optimal printability conditions.

Conclusion

In this work we aimed to expand the range of materials available for stereo-lithography printing and reduce our dependence on petroleum-derived resins. Novel sustainable materials based on poly(glycerol) 4 and 6 (meth)acrylates were developed and optimised for SLA. The printability of these materials was opti-mised and tested *via* the printing of numerous scaffolds, showcasing good resolution and fidelity. When appropriately post-processed, they could also be rendered biocompatible. This work showed that it was possible to print with renewable source materials that were produced in a sustainable, scalable, and atom-efficient synthetic route. To further push the sustainability of PG-based materials for SLA, polyglycerols were functionalised with maleate and norbor-nene groups *via* a ring-opening one-step reaction, as maleic anhydride and nor-bornene anhydride can be fully bioderived. Norbornene-based polymers for AM have been previously utilised for bio-instructive purposes, opening up another application for these sustainable materials. A screening of these materials showed that by utilising a thiol crosslinker, these materials could be cured in a timeframe compatible with SLA. This work has shown that polyglycerols are an optimal backbone for the production of renewable materials for SLA as they have ideal physical and chemical properties, such as optimal viscosity, translucency and biocompatibility, and importantly have the ability to be easily functionalised with

a variety polymerisable moieties. In the future, this strategy could be used to produce a library of sustainable and functional materials for SLA.

Data availability

The data supporting this article have been included as part of the ESI.† Further data is available upon request to the authors.

Conflicts of interest

There are no conflicts to declare.

Acknowledgements

References

1 T. D. Ngo, A. Kashani, G. Imbalzano, K. T. Q. Nguyen and D. Hui, *Composites, Part B*, 2018, **143**, 172–196.

2 Y. Wu, J. Fang, C. Wu, C. Li, G. Sun and Q. Li, *Int. J. Mech. Sci.*, 2023, **246**, 108102.

3 W. Li, M. Wang, H. Ma, F. A. Chapa-Villarreal, A. O. Lobo and Y. S. Zhang, *iScience*, 2023, **26**, 106039.

4 X. Wang, M. Jiang, Z. Zhou, J. Gou and D. Hui, *Composites, Part B*, 2017, **110**, 442–458.

5 Y. Wu, J. Fang, C. Wu, C. Li, G. Sun and Q. Li, *Int. J. Mech. Sci.*, 2023, **246**, 108102.

6 M. Abbasi, P. Váz, J. Silva and P. Martins, *Appl. Sci.*, 2025, **15**, 2245.

7 M. Pagac, J. Hajnys, Q. P. Ma, L. Jancar, J. Jansa, P. Stefek and J. Mesicek, *Polymers*, 2021, **13**, 598.

8 E. M. Maines, M. K. Porwal, C. J. Ellison and T. M. Reineke, *Green Chem.*, 2021, **23**, 6863–6897.

9 E. Sanchez-Rexach, T. G. Johnston, C. Jehanno, H. Sardon and A. Nelson, *Chem. Mater.*, 2020, **32**, 7105–7119.

10 M. Hassan, A. K. Mohanty and M. Misra, *Mater. Des.*, 2024, **237**, 112558.

11 H. Sardon, T. Long and H. Le Ferrand, *ACS Sustain. Chem. Eng.*, 2022, **10**, 1983–1985.

12 J. T. Sutton, K. Rajan, D. P. Harper and S. C. Chmely, *ACS Appl. Mater. Interfaces*, 2018, **10**, 36456–36463.

13 V. Chiaradia, E. Pensa, T. O. Machado and A. P. Dove, *ACS Sustain. Chem. Eng.*, 2024, **12**, 6904–6912.

14 A. Firmanda, K. Syamsu, Y. W. Sari, J. Cabral, D. Pletzer, B. Mahadik, J. Fisher and F. Fahma, *Mater. Chem. Front.*, 2022, **6**, 254–279.

15 C. C. Chong, A. Aqsha, M. Ayoub, M. Sajid, A. Z. Abdullah, S. Yusup and B. Abdullah, *Environ. Technol. Innovation*, 2020, **19**, 100859.

16 A. Di Nardo, G. Landi, G. Luciani, M. Portarapillo, G. Ruoppolo, D. Russo, A. Zarrelli and A. Di Benedetto, *Chem. Eng. J.*, 2024, **500**, 156634.

17 C. R. Chilakamarry, A. M. M. Sakinah, A. W. Zularisam and A. Pandey, *Syst. Microbiol. Biomanuf.*, 2021, **1**, 378.

18 M. Elsayed, M. Eraky, A. I. Osman, J. Wang, M. Farghali, A. K. Rashwan, I. H. Yacoub, D. Hanelt and A. Abomohra, *Environ. Chem. Lett.*, 2023, **22**, 609–634.

19 A. Thomas, S. S. Müller and H. Frey, *Biomacromolecules*, 2014, **15**, 1935–1954.

20 (132c) Etherification of Glycerol and Other Biomass-Derived Polyols: New Routes to Valuable Bulk Chemicals | AIChE, **https://proceedings.aiche.org/conferences/aiche-annual-meeting/2009/proceeding/paper/132c-etherification-glycerol-and-other-biomass-derived-polyols-new-routes-valuable-bulk-chemicals**, accessed 18 March 2025.

21 J. Kaur, A. K. Sarma, M. K. Jha and P. Gera, *Biotechnol. Rep.*, 2020, **27**, e00487.

22 E. Krumins, J. C. Lentz, B. Sutcliffe, A. Sohaib, P. L. Jacob, B. Brugnoli, V. Cuzzucoli Crucitti, R. Cavanagh, R. Owen, C. Moloney, L. Ruiz-Cantu, I. Francolini, S. M. Howdle, M. Shusteff, F. R. A. J. Rose, R. D. Wildman, Y. He and V. Taresco, *Green Chem.*, 2024, **26**, 1345–1355.

23 D. J. Whyte, E. H. Doeven, A. Sutti, A. Z. Kouzani and S. D. Adams, *Addit. Manuf.*, 2024, **84**, 104094.

24 A. Mannu and A. Mele, *Catalysts*, 2024, **14**, 931.

25 K. Bandzierz, L. Reuvekamp, J. Dryzek, W. Dierkes, A. Blume and D. Bielinski, *Materials*, 2016, **9**, 607.

26 Z. Weng, X. Huang, S. Peng, L. Zheng and L. Wu, *Nat. Commun.*, 2023, **14**, 1–9.

27 K. Wang, W. Pan, Z. Liu, T. J. Wallin, G. van Dover, S. Li, E. P. Giannelis, Y. Menguc and R. F. Shepherd, *Adv. Mater.*, 2020, **32**, 2001646.

28 Rheology of our 3Dresyns, **https://www.3dresyns.com/pages/rheological-aspects-of-our-3dresyns**, accessed 2 April 2025.

29 Z. Weng, X. Huang, S. Peng, L. Zheng and L. Wu, *Nat. Commun.*, 2023, **14**, 1–9.

30 L. Y. Wong, S. Ganguly and X. S. Tang, *Polymer*, 2024, **307**, 127305.

31 D. K. Patel, H. Sakhaei, M. Layani, B. Zhang, Q. Ge, S. Magdassi, D. K. Patel, S. Magdassi, A. H. Sakhaei, B. Zhang, Q. Ge and M. Layani, *Adv. Mater.*, 2017, **29**, 1606000.

32 Z. Weng, X. Huang, S. Peng, L. Zheng and L. Wu, *Nat. Commun.*, 2023, **14**, 1–9.

33 M. Suh, D. Proctor, G. Chappell, J. Rager, C. Thompson, S. Borghoff, L. Finch, R. Ellis-Hutchings and K. Wiench, *Toxicology*, 2018, **402–403**, 50–67.

34 R. Zhu, A. Chatzidimitriou, B. Liu, D. J. Kerwood and J. Q. Bond, *ACS Catal.*, 2020, **10**, 1555–1565.

35 R. Cucciniello, D. Cespi, M. Riccardi, E. Neri, F. Passarini and F. M. Pulselli, *Green Chem.*, 2023, **25**, 5922–5935.

36 R. Wojcieszak, F. Santarelli, S. Paul, F. Dumeignil, F. Cavani and R. V Gonçalves, *Sustainable Chem. Processes*, 2015, **3**, 1–11.

37 H. Li, X. Liu, Y. Xiao and K. Cao, *Chem. Eng. J.*, 2024, **498**, 155561.

38 C. E. Hoyle, C. N. Bowman, C. N. Bowman and C. E. Hoyle, *Angew. Chem., Int. Ed.*, 2010, **49**, 1540–1573.

39 D. Gong, Q. Lin, Z. Shao, X. Chen and Y. Yang, *RSC Adv.*, 2020, **10**, 27225–27234.

40 Y. Liu, H. L. Cater, E. A. Recker and Z. A. Page, *Chem. Commun.*, 2025, **61**, 3860–3863.

41 A. Dobos, J. Van Hoorick, W. Steiger, P. Gruber, M. Markovic, O. G. Andriotis, A. Rohatschek, P. Dubruel, P. J. Thurner, S. Van Vlierberghe, S. Baudis and A. Ovsianikov, *Adv. Healthcare Mater.*, 2020, **9**, 1900752.

42 M. L. Lepage, G. Alachouzos, J. G. H. Hermens, N. Elders, K. J. van den Berg and B. L. Feringa, *J. Am. Chem. Soc.*, 2023, **145**, 17211–17219.

43 E. Çakmakçi, B. Yuce-Dursun and S. Demir, *React. Funct. Polym.*, 2017, **111**, 38–43.

44 J. Sherwood, M. De bruyn, A. Constantinou, L. Moity, C. R. McElroy, T. J. Farmer, T. Duncan, W. Raverty, A. J. Hunt and J. H. Clark, *Chem. Commun.*, 2014, **50**, 9650–9652.

45 C. Roussel, V. Marchetti, A. Lemor, E. Wozniak, B. Loubinoux and P. Gérardin, *Holzforschung*, 2001, **55**, 57–62.

46 D. F. Martínez-Martínez, J. J. Beltrán-Morales, M. A. Noriega-Valencia and P. C. Narváez-Rincón, *Chem. Eng. Res. Des.*, 2023, **198**, 46–55.

47 X. Xiao, Z. Huang, X. Jiang, Y. Yang, L. Yang, S. Yang, C. Niu, Y. Xu and L. Feng, *Polymer*, 2022, **245**, 124696.

48 S. M. Hong, O. Y. Kim and S. H. Hwang, *RSC Adv.*, 2021, **11**, 34263.